

## EXPERIMENTAL ANALYSIS ON WEDM OF MONEL 400 ALLOYS IN A RANGE OF THICKNESSES

Gurusamy Selvakumar, Soumya Sarkar, Souren Mitra

Jadavpur University, Production Engineering Department,  
188, Raja Subodh Chandra Mullik Road, Kolkata – 700032, West Bengal (State), India

Corresponding author: Gurusamy Selvakumar, selvakumaratju@gmail.com

**Abstract:** The experimental analysis presented in this paper aims at the selection of optimal machining conditions for wire electrical discharge machining (WEDM) of Monel 400 alloy. The workpiece thickness has been cleverly considered as control factor along with the pulse on time, pulse frequency and peak current and its effects on the material removal rate and the surface roughness has been investigated with the minimum number of experiments. The dimensional shift for every machining condition has been predicted and inputted to CNC system as wire offset value to enhance the dimensional accuracy of the product. This work has been established through response surface methodology (RSM). The analysis of variance (ANOVA) and verification experiments have been performed to test the adequacy of the RSM models. Based on the Pareto optimality approach, the material removal rate and the surface roughness were concurrently optimized to produce optimal technology guidelines for any job thickness ranging 3mm to 23mm.

**Key words:** WEDM, Monel 400 alloy, job thickness, RSM, optimization, Technology guidelines.

### 1. INTRODUCTION

Monel 400 is an outstanding alloy among all commonly used engineering materials for its corrosion resistance, toughness and cryogenic properties. It is used in many industries such as ship building, nuclear, aerospace, missile, ultrasonic machine tools, pharmacy, petroleum, chemical, pumps, shafts and valve industries. The conventional machining of this alloy is very difficult as it has a tendency to work hardening. Work hardening leads to cutting tool failure and results in poor process performance. Wire Electrical Discharge Machining (WEDM) is one of the promising machining methods to process Monel 400 alloy (chemical composition by weight %: 0.047C, 0.172 Si, 1.03 Mn, 0.012 P, 0.01 S, 0.1 Cr, 0.1 Mo, 1.66 Fe, 0.029 V, 0.1 W, 29.24 Cu, 0.01 Al, 0.103 Co, 0.1 Nb, 0.047 Ti, 0.031 Mg, and 67.4 Ni) to any complex shape with very high precision and accuracy. In WEDM, there is no relative contact between the tool and the workpiece material that makes it free from work hardening. The selection of optimum machining parameters for obtaining higher material removal rate with specified

surface finish and other accuracy features is a difficult job in WEDM due to the stochastic nature of the process involving a huge number of process variables. Many attempts have been made on setting of optimal process parameters to maximize cutting speed on various materials other than Monel 400. Kuriakose & Shunmugam (2005), Prasad & Gopala Krishna (2009) optimized the WEDM responses through Non-dominated sorting genetic algorithm (NSGA). Sarkar et al.,(2005, 2006) produced a technology guideline for optimum machining of gamma titanium aluminide based on Pareto-optimal solutions. Additionally, they calculated the wire offset value and used it as input parameter to enhance the dimensional accuracy of the product. By applying multi response signal-to-noise (MRSN) ratio technique, Ramakrishnan & Karunamoorthy (2006, 2008) reported optimal setting for WEDM of tool steel and inconel 718. Tosun et al.,(2004) investigated the effects of WEDM parameters on the kerf (cutting width). Huang & Liao (2003) proposed grey relational analysis for optimization. Based on response surface methodology (RSM), Hewidy et al., (2005) proposed best working condition for each response namely the material removal rate, wear ratio and surface roughness. Chen et al., (2010) presented an optimal setting by employing back-propagation neural network model for prediction and simulated annealing algorithm for optimization. Portillo et al., (2009) employed Artificial Neural Networks (ANN) model to detect the degradation of the WEDM process in a range of steel workpiece thicknesses (50-100 mm). Rajurkar et al., (1997) developed a WEDM adaptive control system that optimizes the on-line sparking frequency by estimating the work piece height. Liao et al.,(2002) used ANN model for the on-line estimation of the workpiece height in WEDM.

Previous literatures reporting into the optimization of WEDM are reviewed in order to highlight the novelty of the present work. Except a few (Portillo et al., 2009, Rajurkar et al., 1997, Liao et al.,2002), most of the researchers have conducted study on one fixed workpiece thickness. In the proposed work, job

thickness has been considered along with other sparking factors to study the influence of the same on the responses. The consideration of workpiece thickness as parameter is a clever approach that drastically reduces the cost of experimentation to find optimal setting in a range of thicknesses. Ramakrishnan & Karunamoorthy (2006, 2008), Nihat Tosun et al., 2004, Huang & Liao (2003), Hewidy et al., 2005 and Chen et al., 2010 have proposed single optimal setting for every response. This outcome did not have any industrial value as there is a need to select appropriate parameters to achieve maximum material removal rate (productivity) with customer specified surface finish and other accuracy features. In practical point of view, a set of optimal machining conditions proposed by Kuriakose & Shunmugam 2005, Prasad & Gopalakrishna 2009, Sarkar et al., (2005, 2006) are significant in selecting parameters according to customer requirements. In the present work, responses are concurrently optimized by following Sarkar et al., (2005), through Pareto-optimality approach for all workpiece thickness ranging from 3mm to 23 mm. The optimal machining conditions reported in this work have ample industrial applications because of the versatility of Monel 400 alloy.

## 2. EXPERIMENTAL DESIGN

Experiments were performed on an Electra Supercut 734 series 2000 CNC Wirecut-EDM machine. Based on the literature survey and the trial experiments, the control factors namely pulse on time (A), pulse frequency (B), peak current (C) and job thickness (D) and its levels have been selected as shown in Table 1. The pulse frequency indicates the number of sparks applied per second and is the reciprocal of the sum of pulse on time and pulse off time. There are other factors, which would have an effect on the measure of performance are kept constant i.e. product shape and size (rectangle of size 8 mm × 5 mm), wire electrode (0.25 mm diameter brass), workpiece material (Monel 400 alloy), dielectric fluid (distilled water), temperature of the dielectric (28° C), conductivity of the dielectric (20 mho), dielectric flushing pressure (8.5 kg/cm<sup>2</sup>), Servo voltage (9V), Servo feed setting (Proportional mode - 0090), peak voltage (100 V), wire feed rate (6 m/min), wire tension (900 grams), threshold setting (60%) and angle of cut (vertical).

In this paper, cutting performance of WEDM is measured by material removal rate (mm<sup>2</sup>/min) and surface roughness  $R_a$  ( $\mu$ m). The actual job profile (punch) produced in WEDM is undersized by half of the width of the cut as illustrated in Fig.1. This deviation in dimension is named as dimensional shift and expresses in equation 1.

$$\text{Dimensional shift (DS)} = 0.5x (w_p - w_a) \quad (1)$$

Where  $w_p$  is the width of the programmed path and  $w_a$  is width of the actual job profile.  $w_a$  was measured by using Mitutoyo, Japan make digital micrometer having least count of 0.001mm.

Table 1. Control factors and their levels

S.no	Control factor	Symbol	Levels					Unit
			-2	-1	0	1	2	
1	pulse on time	A	0.35	0.65	0.95	1.25	1.55	$\mu$ s
2	pulse frequency	B	37.1	44.525	51.95	59.375	66.8	KHz
3	peak current	C	60	90	120	150	180	A
4	job thickness	D	3	8	13	18	23	mm

The deviation of the actual job dimension from the required (programmed) dimension can be eliminated by predicting dimension shift for every parameter setting and inputted to CNC system as wire offset (wire compensation) value. All the experiments were conducted with zero wire offset setting and the dimensional shifts have been measured along with material removal rate and surface roughness. During modeling, the dimensional shift has been considered as response parameter in order to predict its value at various control settings. But in the context of actual machining, it has been considered as input parameter and incorporated in CNC part programme as wire offset to enhance the dimensional accuracy of the machined part (Sarkar et al., 2005).

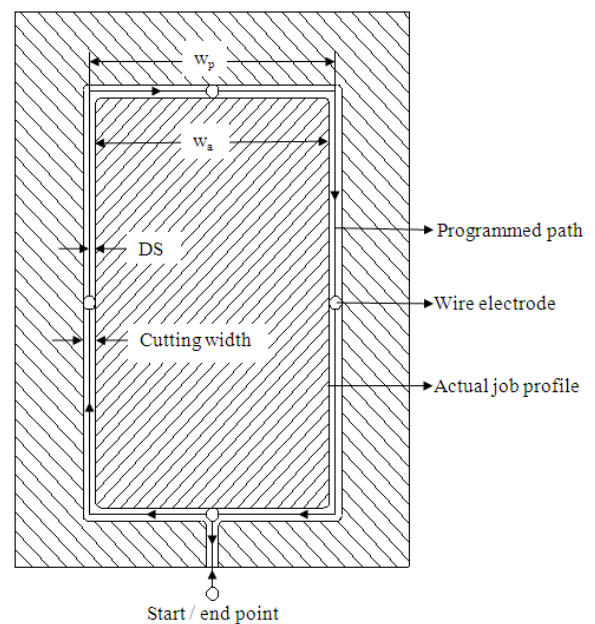


Fig. 1. Programmed path and actual job profile

Based on the input factors and their levels listed in Table 1, a uniform-precision rotatable central composite experimental design for the modeling of the Wire EDM process is shown in Table 2. This design consists of 16 factorial runs, 8 axial runs as

well as 7 central runs. The experimental runs are performed randomly (i.e. not following the order illustrated in the 1<sup>st</sup> column of Table 2). Further, another set of experiment as shown in Table 3 has been carried out to test the model against new input data. The set of input parameter combinations used for this purpose are different from that of Table 2.

Table 2. Experimental results based on uniform rotatable central composite experimental design

Experiment number	Input parameters				Responses		
	Pulse on time ( $\mu$ s)	Pulse frequency (KHz)	Peakcurrent (Amps)	Job thickness (mm)	Material removal rate ( $\text{mm}^2/\text{min}$ )	Surface roughness ( $\mu\text{m}$ )	Dimensional shift ( $\mu\text{m}$ )
	A	B	C	D	MRR	$R_a$	DS
1	0.65	44.525	90	8	4.86	1.529	132
2	1.25	44.525	90	8	11.48	2.008	135
3	0.65	59.375	90	8	5.05	1.505	127
4	1.25	59.375	90	8	12.17	1.969	145
5	0.65	44.525	150	8	5.53	1.525	136
6	1.25	44.525	150	8	14.00	2.136	138
7	0.65	59.375	150	8	5.84	1.569	127
8	1.25	59.375	150	8	18.25	2.197	147
9	0.65	44.525	90	18	5.00	1.517	143
10	1.25	44.525	90	18	12.00	1.974	130
11	0.65	59.375	90	18	4.86	1.477	156
12	1.25	59.375	90	18	13.73	1.995	159
13	0.65	44.525	150	18	5.87	1.467	141
14	1.25	44.525	150	18	15.88	1.948	128
15	0.65	59.375	150	18	5.34	1.484	151
16	1.25	59.375	150	18	15.33	1.922	153
17	0.35	51.95	120	13	2.30	0.683	138
18	1.55	51.95	120	13	19.44	2.131	143
19	0.95	37.1	120	13	7.45	1.847	128
20	0.95	66.8	120	13	9.66	1.789	147
21	0.95	51.95	60	13	5.98	1.665	151
22	0.95	51.95	180	13	12.84	1.871	152
23	0.95	51.95	120	3	8.18	1.997	134
24	0.95	51.95	120	23	8.66	1.749	150
25	0.95	51.95	120	13	8.00	1.770	148
26	0.95	51.95	120	13	8.13	1.848	151
27	0.95	51.95	120	13	10.24	1.872	149
28	0.95	51.95	120	13	8.71	1.782	150
29	0.95	51.95	120	13	9.62	1.778	150
30	0.95	51.95	120	13	9.49	1.746	152
31	0.95	51.95	120	13	8.45	1.761	149

For each experimental run, the specified input parameter combination was set and the workpiece was machined. The cutting speed ( $\text{mm}/\text{min}$ ) was recorded directly from the monitor of the machine and the MRR ( $\text{mm}^2/\text{min}$ ) was computed by multiplying thickness of the job with the monitor readings. Surface roughness was measured by using perthometer manufactured by Mahr, Germany. The dimensional shift (wire offset) values were calculated

by measuring the finished job dimension with the aid of a digital micrometer.

Table 3. Verification experiment

Experiment number	Input parameters				Responses		
	Pulse on time ( $\mu$ s)	Pulse frequency (KHz)	Peakcurrent (Amps)	Job thickness (mm)	Material removal rate ( $\text{mm}^2/\text{min}$ )	Surface roughness ( $\mu\text{m}$ )	Dimensional shift ( $\mu\text{m}$ )
	A	B	C	D	MRR	$R_a$	DS
1	0.95	66.8	120	8	9.45	1.815	124
2	1.55	59.375	60	18	14.67	1.796	145
3	1.25	59.375	90	13	14.17	2.018	150
4	0.65	44.525	180	13	5.92	1.521	154
5	1.25	44.525	90	3	9.06	2.363	123
6	0.65	59.375	150	3	5.82	1.676	120

### 3. RSM MODELING OF WEDM

Response surface methodology (RSM) is a combination of mathematical and statistical techniques useful for modeling and analyzing the problem in which several independent variables influence a dependent variable or response (Montgomery, 1997). RSM also quantifies relationships among one or more measured responses and the vital input factors. The relationship between the WEDM control factors and the responses namely material removal rate (MRR), surface roughness ( $R_a$ ) and dimensional shift (DS) has been established using a second-order polynomial response surface mathematical model as presented in equations 2-4. As the material removal rate and the surface roughness are the true responses in determining the performance of WEDM, the effects of control factors on them are studied using equation 2 and 3. The equation 4, stands for dimension shift is used only for prediction and the predicted values are passed to CNC programme to enhance the dimensional accuracy of the product.

$$y(\text{MRR}) = 5.34967 - 16.1836A + 0.028726B - 0.0769638C + 0.628692D + 6.05142A^2 - 0.000618930B^2 + 0.00019959C^2 - 0.00271488D^2 + 0.176487AB + 0.0782639AC + 0.0520833AD + 0.0002834BC - 0.0082997BD - 0.001346CD \quad (2)$$

$$y(R_a) = 0.853854 + 2.77024A - 0.0318224B - 0.0005844C + 0.00704991D - 0.986872A^2 + 0.000252701B^2 + 1.590608 \times 10^{-6} C^2 + 0.00110726D^2 + 0.000561167AB + 0.00166667AC - 0.012AD + 0.0000499BC - 0.000118BD - 0.0002325CD \quad (3)$$

$$y(\text{DS}) = -12.9536 + 3.56407A + 4.36384B + 0.295392C + 0.774221D - 30.3902 A^2 - 0.06322B^2 + 0.0000165C^2 - 0.0944D^2 + 1.79574 AB - 2.66667AD - 0.00337 BC + 0.121212BD - 0.01CD \quad (4)$$

Where,  $y(\text{MRR})$ ,  $y(R_a)$  and  $y(\text{DS})$  stands for material removal rate, surface roughness and dimensional shift respectively. A, B, C and D represents input parameters namely pulse on time, pulse frequency, peak current and job thickness.

The analysis of variance (ANOVA) was used to check the adequacy of the developed models. Table 4 shows the summary of ANOVA. From Table 4, it is observed that the p-value for the model was lower than 0.05 (i.e. at 95% confidence level) which indicates that the proposed model (equation 2-4) is statistically significant. The other important coefficient  $R^2$ , which is called determination coefficient in the resulting ANOVA table, is defined as the ratio of the explained variation to the total variation, is a measure for degree of fit. When  $R^2$  approaches to unity, the response model fits better to the actual data and shows less difference between the predicted and actual values. The  $R^2$  value for MRR,  $R_a$ , and the dimensional shift are 97.6%, 95.7% and 98.2% respectively as indicated in Table 4. Further, the  $R^2_{(\text{adj})}$  is account for the number of predictions in the model. The values of adjusted  $R^2$  ( $R^2_{(\text{adj})} = 95.4\%$  for MRR, 92% for  $R_a$  and 96.6% for dimensional shift) indicates the goodness of the model.

Table 4. Summary of ANOVA for developed models

Response	P-value	$R^2$	$R^2_{(\text{adj})}$
Material removal rate (MRR)	0	97.6%	95.4%
Surface roughness( $R_a$ )	0	95.7%	92%
Dimensional shift (DS)	0	98.2%	96.6%

Apart from routine adequacy checking, the model was tested against another set of test data to check the prediction performance of the model. The experimental results presented in Table.3 are compared with the corresponding RSM model predictions as illustrated in Table 5. It is found that the prediction errors are not high and the prediction performance of the model is quite satisfactory. The prediction error illustrated in Table 5 has been defined as:

$$\text{Prediction error (\%)} = \left| \frac{\text{Experimental value} - \text{Predicted value}}{\text{Experimental value}} \right| \times 100 \quad (5)$$

Table 5. Comparison of RSM model prediction with the experimental result

S.no	RSM model prediction			Prediction error (%)		
	MRR (mm <sup>2</sup> /min)	$R_a$ ( $\mu\text{m}$ )	DS ( $\mu\text{m}$ )	MRR	$R_a$	DS
1	10.15	1.925	130	7.41	6.08	4.84
2	16.52	1.907	155	12.61	6.17	6.90
3	12.79	1.953	155	9.74	3.19	3.33
4	6.79	1.445	143	14.70	5.01	7.14
5	9.67	2.146	131	6.73	9.19	6.50
6	6.70	1.698	110	15.12	1.32	8.33
Average prediction error (%)				11.05	5.16	6.17

## 4. RESULTS AND DISCUSSION

### 4.1. Parametric influence on material removal rate (MRR)

Material removal rate is an imperative response in determining the productivity of the WEDM process. The effects of various process parameters on MRR have been analyzed through RSM model presented in equation .2. The variation of MRR with the pulse on time and peak current for a fixed job thickness and pulse frequency is graphed in Fig.2. The energy content of a single spark discharge is the product of pulse on time and peak current. Therefore, increase in pulse on time or peak current produces higher energy pulses that melt and vaporize higher amount of workpiece material. Due to this, the MRR increases with the pulse on time and the peak current as depicted in Fig.2.

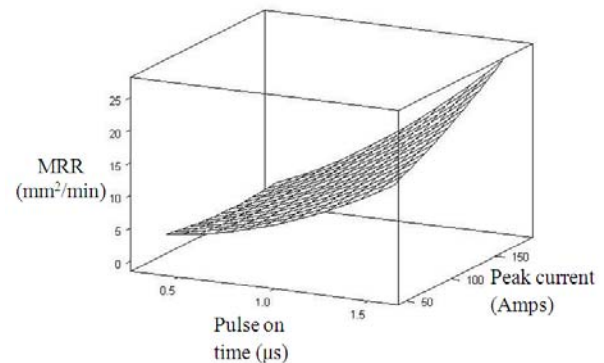


Fig. 2. Effect of pulse on time and peak current on MRR for fixed pulse frequency of 51.95 KHz and Job thickness of 13mm

For a fixed pulse on time and peak current, the MRR is proportional to the pulse frequency, gap voltage and the pulse energy utilization efficiency ( $\eta$ ). The pulse energy utilization efficiency is the ratio between the energy observed by the workpiece to the sum of energy observed by the workpiece and the dielectric medium.

Fig.3 shows the MRR is increasing with the pulse frequency as it defines the number of sparks applied per second. During experimentation, it is observed that the increase in job thickness decreases the gap

voltage that consequently reduces the gap width. Therefore, increase in job thickness increases the MRR through increase in pulse energy utilization efficiency manifested by reduction in gap width and decreases the MRR due to decrease in gap voltage.

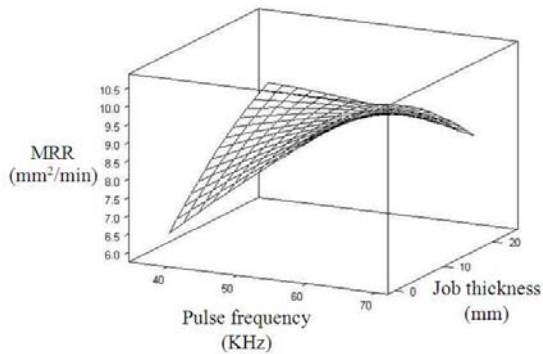


Fig. 3. Effect of pulse frequency and Job thickness on MRR for fixed pulse on time of  $0.95\mu\text{s}$  and peak current of 120 Amps

In the lower frequency region of Fig.3, the material removal rate linearly increases with the job thickness. This is attributed by the predominant raise in pulse energy utilization efficiency than the decrease in cutting speed caused by gap voltage. At the higher frequency region, the material removal rate increases up to certain thickness and later it decreases in a non linear fashion. This is due to the combined effect of decrease in gap voltage and the gap width. For a particular frequency value, initial increase in workpiece thickness enhances the MRR as the rate of increase of pulse energy utilization efficiency is higher than the rate of decrease of gap voltage. After certain thickness, the rate of decrease of later is higher than the rate of increase of the former. Hence, the MRR decreases.

#### 4.2 Parametric influence on surface roughness ( $R_a$ )

Based on equation 3, the effect of various machining parameters on the surface roughness ( $R_a$ ) has been analyzed. Fig.4 shows the surface roughness is non-linearly increases with the pulse on time and peak current for a preset pulse frequency and job thickness. The increase in pulse on time or peak current produces higher energy pulses that evaporate more quantity of workpiece material by producing higher depth of crater. Due to this,  $R_a$  increases (i.e. the surface finish quality deteriorates) with the pulse on time and the peak current.

Fig.5 illustrates the influence of pulse frequency and job thickness on surface roughness for a preset pulse on time of  $0.95\mu\text{s}$  and peak current of 120 Amps. The Figure demonstrates that for a particular workpiece thickness, increase in pulse frequency decreases the surface roughness ( $R_a$ ) value. This is due to the rapid production of constant energy pulse (as the pulse on

time and peak current are kept constant) that applied in a homogeneous manner among the workpiece and the wire electrode.

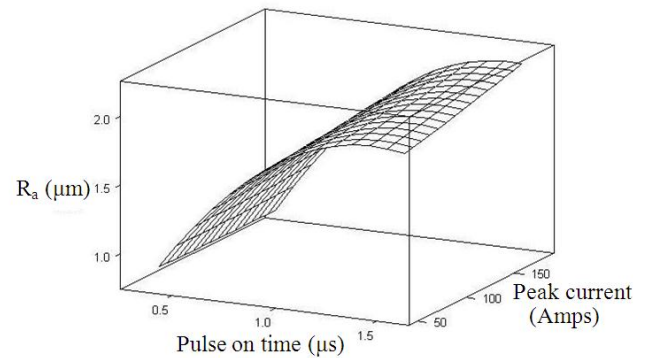


Fig. 4. Effect of pulse on time and peak current on  $R_a$  for fixed pulse frequency of 51.95 KHz and Job thickness of 13mm

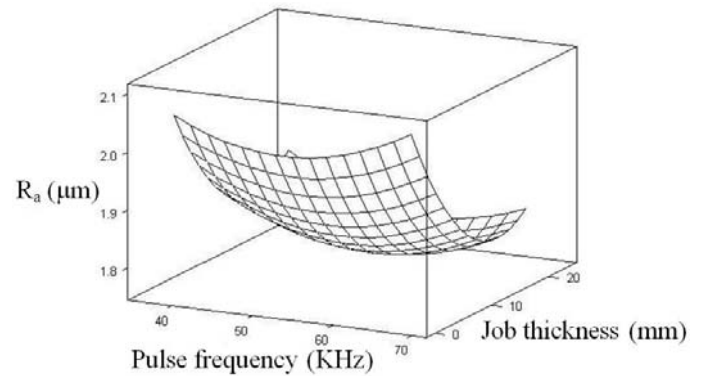


Fig. 5. Effect of pulse frequency and Job thickness on  $R_a$  for fixed pulse on time of  $0.95\mu\text{s}$  and peak current of 120 Amps

As discussed earlier, increase in job thickness reduces the cutting speed owing to decrease in gap voltage. The reduced cutting speed allows enough time for uniform vaporization of the workpiece material. Due to this, the depth of the crater reduced and hence the  $R_a$  value. Meanwhile decrease in gap width manifested by higher job thickness enhances the pulse energy utilization efficiency, is also reduces  $R_a$ . The gap width reduction is small due to control action and as such it is not a governing factor in determining the surface roughness value. For this reason there is a drop in surface roughness value predominantly with increase in job height.

#### 5. PARAMETRIC OPTIMIZATION THROUGH PARETO OPTIMALITY APPROACH

The material removal rate and surface roughness are conflicting in nature. Therefore, there is hardly any possibility of having a single optimal setting for both the responses. However, it is possible to consider the multi-objective optimization problem into a single objective problem by combining the individual objective functions by assigning suitable weights

(Ramakrishnan&Karunamoorthy (2006, 2008), Tosun et al.,2004 , Huang&Liao 2003 , Hewidy et al.,2005 and Chen et al.,2010). In practice, it is very difficult to select these weights even for a field expert. In addition, optimizing a particular problem with respect to a single objective can produce undesirable results with respect to the other objectives.

The second general approach is searching for Pareto optimal solution set or Pareto front. There will be a set of optimal trade-offs between the conflicting objectives. A Pareto optimal set is a set of solutions that are non-dominated with respect to one another. While moving from one Pareto solution to another, there is always a certain amount of importance in one objective to achieve a certain amount of gain in the other. Generating the Pareto set has several advantages such as it allows the user to make an informed decision by seeing a wide range of options. This was ignored by the former method. Therefore, this approach is considered as superior to the previous method especially for manufacturing industries involved in producing components with the specified surface roughness.

The pulse on time, pulse frequency, and peak current are respectively having 25, 11, and 13 discrete values among the levels considered. The thickness of the job can take any value from 3mm to 23mm. In order to simplify the optimization problem, 5 distinct thicknesses as stated in Table 1 has been considered. Therefore, totally 17,875 (25 x 11 x 13 x 5 = 17,875) combination of control parameters are available for machining among which the most suitable combination needs to be selected according to the requirement.

The responses i.e. MRR and surface roughness, were predicted for all possible combinations of the input factors by using equation 2 and 3. Pareto based non-dominated sorting scheme proposed by Deb et al., (2002) has been applied to rank all (17,875) machining combinations. The identically ranked Pareto-optimal solutions are equally significant as far as surface roughness and MRR are concerned. Fig.6 depicts the non-dominated solutions (rank 1 solutions) marked by asterisks along with the inferior solutions in the objective space. There are totally 115 machining combinations have been ranked 1 and are graphed in Fig.7. In optimization point of view it is plausible to list the rank 1 combination by keeping job thickness as a control factor. But in production point of view, it has no significance. For instance, a customer demands an intricate shape of 8mm thickness with  $R_a \leq 1 \mu\text{m}$ . In this circumstance, the WEDM operator cannot get any fruitful information from the results depicted in Fig.7. Since, there are only two non-dominated solutions such as: (i) the pulse on time of  $1.55\mu\text{s}$ , pulse frequency of 62.305 KHz, and Peak current of 180 Amps yields the MRR of  $28.289 \text{ mm}^2/\text{min}$  and  $R_a$  of  $2.3856 \mu\text{m}$  and (ii) Pulse on time of  $1.55\mu\text{s}$ , pulse frequency of

64.309 KHz, and Peak current of 180 Amps yields the MRR of  $28.703 \text{ mm}^2/\text{min}$  and  $R_a$  of  $2.4038 \mu\text{m}$  are made available to the user.

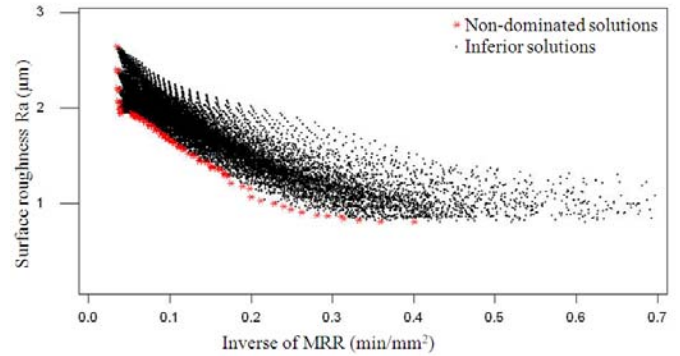


Fig. 6. Non-dominated (Rank 1) solutions along with inferior solutions in the response space

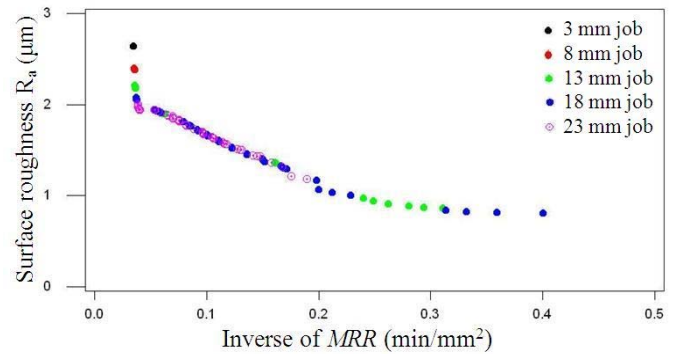


Fig. 7. Non-dominated solutions in response space

Therefore, according to the workpiece thickness, the total machining combinations (17,875) have been clustered into 5 groups to produce technology guideline for optimal machining of Monel 400 alloy. Now, each group representing a particular thickness will have 3,575 machining combinations. In accordance with equation 2 and 3, the responses MRR and  $R_a$  are calculated. Then, Pareto based non-dominated sorting is applied to rank all (3,575) machining combinations and the rank 1 solution for individual job thickness have been plotted in Fig.8. It is observed that there are 110, 124, 124, 104, and 84 non-dominated solutions existing for individual job thickness of 3mm, 8mm, 13mm, 18mm, and 23mm respectively. These non-dominated solutions are equally important as far as  $R_a$  and MRR are concerned. It is practically plausible to report limited non-dominated solutions by considering  $R_a$  at a regular interval of  $0.1\mu\text{m}$  (approximately). Thus, technology guideline for optimal machining of individual workpiece thickness has been tailored and reported in Table 6. Similar fashion, optimal technology guidelines for any thickness ranging 3mm to 23mm can be produced.

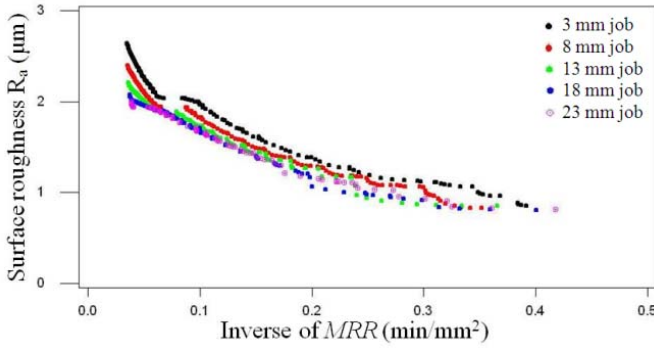


Fig. 8. Non-dominated solutions for individual job thickness

Table 6. Technology table for various job thicknesses

Job thickness : 3 mm						
S.no	Input parameters				Responses	
	Pulse on time (µs)	pulse frequency (KHz)	Peak current (Amps)	Wire offset (µm)	MRR (mm <sup>2</sup> /min)	R <sub>a</sub> (µm)
1	0.35	57.637	60	86	2.55	0.854
2	0.4	57.471	60	90	2.72	0.960
3	0.45	57.307	60	94	2.91	1.062
4	0.35	54.496	170	102	3.36	1.119
5	0.35	65.147	180	73	4.13	1.222
6	0.4	60.976	180	90	4.64	1.301
7	0.45	60.79	180	95	5.32	1.411
8	0.5	60.606	180	99	6.04	1.516
9	0.55	60.423	180	103	6.78	1.616
10	0.6	60.241	180	107	7.55	1.712
11	0.65	60.060	180	111	8.34	1.802
12	0.7	63.694	180	105	9.56	1.920
13	1.55	60.423	60	135	15.57	2.048
14	1.55	64.309	70	134	17.26	2.108
15	1.55	64.309	90	135	19.07	2.203
16	1.55	64.309	110	136	21.04	2.300
17	1.55	60.423	140	141	23.36	2.419
18	1.55	60.423	160	142	25.71	2.515
19	1.55	60.423	180	143	28.21	2.612
20	1.55	64.309	180	140	29.19	2.648
Job thickness: 8mm						
1	0.35	57.637	60	112	2.84	0.825
<b>2</b>	<b>0.35</b>	<b>41.068</b>	<b>60</b>	<b>120</b>	<b>3.17</b>	<b>0.902</b>
3	0.35	61.162	180	108	3.31	1.016
4	0.4	57.471	180	119	3.96	1.106
5	0.45	57.307	180	122	4.63	1.213
6	0.5	54.054	180	129	5.24	1.301
7	0.55	56.980	180	128	6.07	1.413
8	0.6	56.818	180	131	6.83	1.506
9	0.65	60.060	180	128	7.80	1.615
10	0.7	63.694	180	124	8.88	1.727
11	0.75	63.492	180	127	9.78	1.804
12	0.85	59.347	180	138	11.34	1.915
13	1.55	60.423	80	147	17.63	2.013
14	1.55	64.309	100	147	20.09	2.100
15	1.55	64.309	130	147	23.02	2.212
16	1.55	62.305	160	148	25.91	2.310
17	1.55	62.305	180	149	28.29	2.386
18	1.55	64.309	180	148	28.70	2.404
Job thickness : 13 mm						
1	0.35	61.162	60	129	2.73	0.852
2	0.35	44.743	60	135	3.82	0.907
3	0.4	37.879	60	128	4.19	1.071
4	0.45	37.807	60	128	4.24	1.167
5	0.55	48.662	160	143	4.86	1.261
6	0.55	56.980	180	140	5.49	1.289
7	0.6	51.020	160	144	5.51	1.350
8	0.6	64.103	180	133	6.29	1.426
9	0.65	63.898	180	136	7.17	1.511
10	0.75	50.633	180	147	8.56	1.601
11	0.8	59.524	180	146	9.80	1.707
12	0.85	56.022	180	149	10.58	1.754
13	0.9	52.910	180	150	11.33	1.803
14	0.95	52.770	180	150	12.28	1.859
15	1.55	64.309	60	156	16.93	1.907
16	1.55	62.305	100	154	19.72	1.996
17	1.55	56.980	140	148	22.56	2.070
18	1.55	56.980	180	148	26.84	2.163
19	1.55	64.309	180	151	28.09	2.215
Job thickness : 18 mm						
1	0.35	49.14	180	143	2.49	0.804
2	0.35	37.951	180	131	3.18	0.835
3	0.4	44.643	180	140	3.35	0.916
4	0.35	41.068	60	138	4.72	1.031
5	0.4	37.879	60	132	5.04	1.162
6	0.55	48.662	180	145	5.1	1.203
7	0.6	40.65	180	135	5.97	1.307
8	0.65	37.523	180	128	6.66	1.404
9	0.75	48.193	180	146	8.16	1.523
10	0.8	56.18	180	152	9.05	1.605
11	0.85	63.091	180	151	10.03	1.707
12	1	47.619	180	142	12.62	1.811
13	1.05	52.493	180	148	13.86	1.859
14	1.1	55.249	180	150	15.07	1.905
15	1.55	53.908	110	141	19.44	1.954
16	1.55	56.98	180	142	26.39	2.034
17	1.55	60.423	180	146	26.85	2.053
18	1.55	62.305	180	148	27.09	2.066
19	1.55	64.309	180	149	27.34	2.082
Job thickness : 23 mm						
1	0.35	49.140	180	143	1.92	0.807
2	0.35	37.951	160	126	3.11	0.903
3	0.45	40.900	180	130	3.90	1.032
4	0.5	44.444	180	137	4.24	1.112
5	0.6	40.65	180	127	5.82	1.300
6	0.65	48.426	180	142	6.11	1.358
7	0.7	50.761	180	145	6.79	1.432
8	0.75	50.633	180	144	7.63	1.502
9	0.8	37.313	180	111	8.83	1.605
10	0.9	40.161	180	116	10.42	1.703
11	1.05	49.875	180	136	13.30	1.816
12	1.15	58.309	180	148	15.64	1.901
13	1.3	51.813	180	131	18.94	1.943
14	1.55	56.980	180	131	25.81	1.960
15	1.55	64.309	180	143	26.45	2.004

Job thickness: 13 mm						
S.no	Input parameters				Responses	
	Pulse on time (µs)	pulse frequency (KHz)	Peak current (Amps)	Wire offset (µm)	MRR (mm <sup>2</sup> /min)	R <sub>a</sub> (µm)
1	0.35	61.162	60	129	2.73	0.852
2	0.35	44.743	60	135	3.82	0.907
3	0.4	37.879	60	128	4.19	1.071
4	0.45	37.807	60	128	4.24	1.167
5	0.55	48.662	160	143	4.86	1.261
6	0.55	56.980	180	140	5.49	1.289
7	0.6	51.020	160	144	5.51	1.350
8	0.6	64.103	180	133	6.29	1.426
9	0.65	63.898	180	136	7.17	1.511
10	0.75	50.633	180	147	8.56	1.601
11	0.8	59.524	180	146	9.80	1.707
12	0.85	56.022	180	149	10.58	1.754
13	0.9	52.910	180	150	11.33	1.803
14	0.95	52.770	180	150	12.28	1.859
15	1.55	64.309	60	156	16.93	1.907
16	1.55	62.305	100	154	19.72	1.996
17	1.55	56.980	140	148	22.56	2.070
18	1.55	56.980	180	148	26.84	2.163
19	1.55	64.309	180	151	28.09	2.215
Job thickness : 18 mm						
1	0.35	49.14	180	143	2.49	0.804
2	0.35	37.951	180	131	3.18	0.835
3	0.4	44.643	180	140	3.35	0.916
4	0.35	41.068	60	138	4.72	1.031
5	0.4	37.879	60	132	5.04	1.162
6	0.55	48.662	180	145	5.1	1.203
7	0.6	40.65	180	135	5.97	1.307
8	0.65	37.523	180	128	6.66	1.404
9	0.75	48.193	180	146	8.16	1.523
10	0.8	56.18	180	152	9.05	1.605
11	0.85	63.091	180	151	10.03	1.707
12	1	47.619	180	142	12.62	1.811
13	1.05	52.493	180	148	13.86	1.859
14	1.1	55.249	180	150	15.07	1.905
15	1.55	53.908	110	141	19.44	1.954
16	1.55	56.98	180	142	26.39	2.034
17	1.55	60.423	180	146	26.85	2.053
18	1.55	62.305	180	148	27.09	2.066
19	1.55	64.309	180	149	27.34	2.082
Job thickness : 23 mm						
1	0.35	49.140	180	143	1.92	0.807
2	0.35	37.951	160	126	3.11	0.903
3	0.45	40.900	180	130	3.90	1.032
4	0.5	44.444	180	137	4.24	1.112
5	0.6	40.65	180	127	5.82	1.300
6	0.65	48.426	180	142	6.11	1.358
7	0.7	50.761	180	145	6.79	1.432
8	0.75	50.633	180	144	7.63	1.502
9	0.8	37.313	180	111	8.83	1.605
10	0.9	40.161	180	116	10.42	1.703
11	1.05	49.875	180	136	13.30	1.816
12	1.15	58.309	180	148	15.64	1.901
13	1.3	51.813	180	131	18.94	1.943
14	1.55	56.980	180	131	25.81	1.960
15	1.55	64.309	180	143	26.45	2.004

The optimal parameter setting for the earlier instance can be selected from Table 6 (highlighted in bold letters) as pulse on time of 0.35 $\mu$ s, pulse frequency of 41.068 KHz, and Peak current of 60 Amps yields the MRR of 3.17 mm<sup>2</sup>/min and R<sub>a</sub> of 0.902  $\mu$ m. The dimensional shift for this setting is calculated using equation 4 as 120  $\mu$ m. This value is passed to CNC part programme as wire offset value to enhance the dimensional accuracy of the machined part.

## 6. CONCLUSIONS

The experimental investigation presented in this paper proved that WEDM is adequate to machine Monel 400 alloy to any complex shape. The influence of job thickness on the material removal rate and the surface roughness has been studied through RSM model with the minimum cost of experiments. The dimensional accuracy of the product has been improved by predicting dimensional shift and passing the same to the CNC programme as wire off set (wire compensation) value. Using Pareto-optimality approach, optimal technology guidelines for individual job thickness of 3mm, 8mm, 13mm, 18mm and 23 mm have been reported with its industrial utility. The research approach presented in this paper tremendously reduces the cost of experiments and allows the WEDM operator to set the parameter according to the customer demand. The further research in this study might include trim cutting operation to enhance productivity of machining and other surface characteristics.

## ACKNOWLEDGMENT

The authors acknowledge the assistance provided by the CAS Ph-IV Programme of Production Engineering Department, Jadavpur University, under the University Grants Commission, New Delhi. The corresponding author gratefully acknowledges the management of National Engineering College, K.R.Nagar, Tamilnadu, India, for deputing him to pursue research under the QIP scheme of AICTE, New Delhi.

## REFERENCES

- Chen, Hsien-Ching, Lin, Jen-Chang, Yang, Yung-Kuang, Tsai, Chih-Hung., (2010). *Optimization of wire electrical discharge machining for pure tungsten using a neural network integrated simulated annealing approach*, Expert Systems with Applications, 37, 7147–7153.
- Deb, K., Pratap, A., Agarwal, S., Meyarivan, T., (2002). *A Fast and Elitist Multiobjective Genetic Algorithm: NSGA-II*, IEEE Transactions on Evolutionary Computation, 6(2), 182–197.
- Hewidy, M.S., El-Taweel, T.A., El-Safty, M.F., (2005). *Modelling the machining parameters of WEDM of Inconel 601 using RSM*, Journal of Materials Processing Technology, 169, 328–336.
- Huang, J. T., Liao, Y. S., (2003). *Optimization of machining parameters of Wire-EDM based on Grey relational and statistical analyses*, Int. J. Production Research., 41(8), 1707–1720.
- Kuriakose, S., Shunmugam, M.S., (2005). *Multi-objective optimization of WEDM process by Non-Dominated Sorting Genetic Algorithm*, Journal of Materials Processing Technology, 170, 133–141.
- Liao, Y.S., Yan, M.T., Chang, C.C., (2002). *A neural network approach for the on-line estimation of workpiece height in WEDM*, Journal of Materials Processing Technology, 121, 252–258.
- Montgomery, D.C., (1997). *Design and Analysis of Experiments*, 5th ed., pp. 427-500, John Wiley & Sons, Inc., New York.
- Portillo, E., Marcos, M., Cabanes, I., Zubizarreta, A., (2009). *Recurrent ANN for monitoring degraded behaviours in a range of workpiece thicknesses*, Engineering Applications of Artificial Intelligence, 22, 1270-1283.
- Prasad, D.V.S.S.V., Gopala Krishna, A., (2009). *Empirical modeling and optimization of wire electrical discharge machining*, Int. J. Adv. Manuf. Technol., 43, 914–925.
- Rajurkar, K.P., Wang, W.M., Zhao, W.S., (1997). *WEDM-Adaptive Control with a Multiple Input Model for Identification of Workpiece Height*, Annals of the CIRP, 46(1), 147-150.
- Ramakrishnan, R., Karunamoorthy, L., (2006). *Multi response optimization of wire EDM operations using robust design of experiments*, Int. J. Adv. Manuf. Technol., 29, 105–112.
- Ramakrishnan, R., Karunamoorthy, L., (2008). *Modeling and multi-response optimization of Inconel 718 on machining of CNC WEDM process*, Journal of materials processing technology, 207, 343–349.
- Sarkar, S., Mitra, S., Bhattacharyya, B., (2005). *Parametric analysis and optimization of wire electrical discharge machining of  $\gamma$ -titanium aluminide alloy*, Journal of Materials Processing Technology, 159, 286–294.
- Sarkar, S., Mitra, S., Bhattacharyya, B., (2006). *Parametric optimisation of wire electrical discharge machining of  $\gamma$  titanium aluminide alloy through an artificial neural network model*, Int. J. Adv. Manuf. Technol., 27, 501–508.
- Tosun, N., Cogun, C., Tosun, G., (2004). *A study on kerf and material removal rate in wire electrical discharge machining based on Taguchi method*, Journal of Materials Processing Technology, 152, 316–322.